Chinese Medicine

RESEARCH

Open Access

Polyphyllin I exerts anti-hepatocellular carcinoma activity by targeting ZBTB16 to activate the PPARγ/RXRα signaling pathway

Lu shan[1,2†], Yijun Chen[3†], Guo An[4†], Xiaoyu Tao[1], Chuanqi Qiao[1], Meilin Chen[1,2,5], Jiaqi Li[1], Ruichao Lin[1,2*], Jiarui Wu[1*] and Chongjun Zhao[1,2*]

Abstract

Background Studies have reported that polyphyllin I (PPI) had effective anti-tumor activity against hepatocellular carcinoma (HCC). However, the precise molecular mechanism of this action and the direct target remain unclear. The aim of this study was to discover the molecular targets and the exact mechanism of PPI in the treatment of HCC.

Methods Various HCC cells and Zebrafish xenotransplantation models were used to examine the efficacy of PPI against HCC. A proteome microarray, surface plasmon resonance (SPR) analysis, small molecule transfection, and molecular docking were conducted to confirm the direct binding targets of PPI. Transcriptome and Western blotting were then used to determine the exact responding mechanism. Finally, the anticancer effect and its precise mechanism, as well as the safety of PPI, were verified using a mouse tumor xenograft study.

Results The results demonstrated that PPI had significant anticancer activity against HCC in both in vitro studies of two cells and the zebrafish model. Notably, PPI selectively enhanced the action of the Zinc finger and BTB domain-containing 16 (ZBTB16) protein by directly binding to it. Furthermore, specific knockdown of ZBTB16 markedly attenuated PPI-dependent inhibition of HCC cell proliferation and migration caused by overexpression of the gene. The transcriptome and Western blotting also confirmed that the interaction between ZBTB16 and PPI also activated the PPARγ/RXRα pathway. Finally, the mouse experiments confirmed the efficacy and safety of PPI to treat HCC.

Conclusions Our results indicate that ZBTB16 is a promising drug target for HCC and that PPI as a potent ZBTB16 agonist has potential as a therapeutic agent against HCC by regulating the ZBTB16/PPARγ/RXRα signaling axis.

Keywords Polyphyllin I, Hepatocellular carcinoma, ZBTB16, PPARγ/RXRα signaling pathway

†Lu shan, Yijun Chen and Guo An have contributed equally to this work.

*Correspondence:
Ruichao Lin
linrch307@sina.com
Jiarui Wu
exogamy@163.com
Chongjun Zhao
1014256537@qq.com
[1] Department of Clinical Chinese Pharmacy, School of Chinese Materia Medica, Beijing University of Chinese Medicine, Beijing 102488, China
[2] Beijing Key Laboratory for Quality Evaluation of Chinese Materia Medica, School of Chinese Materia Medica, Beijing University of Chinese Medicine, Beijing 102488, China
[3] Institute of Prescriptions and Syndromes, Guangzhou University of Traditional Chinese Medicine, Guangzhou, China
[4] Key Laboratory of Carcinogenesis and Translational Research (Ministry of Education/Beijing), Department of Laboratory Animal, Peking University Cancer Hospital & Institute, Beijing 100142, China
[5] Department of Pharmacy, Jinjiang Municipal Hospital, Quanzhou 362200, Fujian, China

Background

Hepatocellular carcinoma (HCC) is one of the most common malignancies and ranks as the third leading cause of cancer-related death worldwide [1]. China is one of the areas with the highest risk for HCC, contributing 45.3% of all HCC cases worldwide in 2020 [2, 3]. Research has shown that the survival time of over 80% of HCC patients is less than 5 years [4], with surgery currently the first choice and most effective treatment [5]. However, the high recurrence rate for HCC of over 70% over 5 years is the major barrier to prolonging survival and improving the quality-of-life of patients [6]. Traditional Chinese medicine (TCM) has significant advantages in treating HCC [7, 8], with the screening of lead TCM compounds with significant therapeutic effects having great importance for the future development of targeted therapeutic drugs [9].

Zinc finger and BTB domain-containing 16 (ZBTB16, a.k.a. PLZF) is a protein-coding gene that was first identified in a patient with acute promyelocytic leukemia (APL) [10]. The gene codes for zinc finger transcription factors and affects a diverse number of signaling pathways related to the cell cycle, differentiation, and programmed cell death pathways [11–14]. Previous reports have demonstrated that ZBTB16 is under-expressed or silenced in multiple tumor tissues or various cancer types, including HCC [15, 16]. Furthermore, published results have indicated that ZBTB16 in HCC was closely related to the level of alkaline phosphatase in patients while showing good diagnostic value in distinguishing tumors from normal tissues, suggesting its potential as an HCC biomarker [15].

Polyphyllin I (PPI, PubChem CID: 129316759) is an anticancer molecular extracted from Rhizoma Paridis that has significant anticancer effects in various cancers including HCC [17–19]. Despite this, its direct targets and the potential molecular mechanism remain to be elusive. Therefore, it is important to perform comprehensive in-depth research on the mechanisms of PPI, facilitating the development of novel treatments to improve patient outcomes.

The current study investigated the key direct target of PPI using proteomic microarrays that was confirmed using surface plasmon resonance (SPR) analysis. Further investigation was conducted using cell transcriptomics to identify the signaling pathway of PPI that inhibited key direct targets associated with HCC, which was then validated in both in vitro and in vivo experiments. We also evaluated the safety of therapeutic doses of PPI that provided a solid foundation for the development of PPI as a novel targeted cancer treatment drug. The workflow of this study is shown in Fig. 1.

Methods

Cell proliferation assay

The primary HCC cells (Hep3B 2.1–7 and SK-Hep-1) were purchased from Procell (Wuhan, China) and cultured in medium (Procell) supplemented with 10% FBS (Corning, VA, USA) and 1% penicillin–streptomycin (Gibco, Waltham, Massachusetts, USA). The cells were seeded in 96-well culture plates at a density of 1×10^4 cells/well. The next day, 200 mL of fresh medium with different concentrations of PPI (Chengdu Herbpurify Co., Ltd, Chengdu, China) were added to the cells, followed by incubation for 24 h. At the end of the experiment, the cell counting kit-8 (CCK-8; Beyotime, Beijing, China) was used to assess the effect of PPI on cell proliferation, with the absorbance at 450 nm measured in a microplate reader (Synergy H1, Biotek, Vermont, USA) to calculate the dose–effect curve prepared using GraphPad Prism 8.0 (GraphPad Software, La Jolla, USA).

Apoptosis analysis

Based on the results of the CCK8 experiment, the drug concentration for the subsequent in vitro cell experiments was determined to be 2.5 μg/mL (low-dose group, L) and 5 μg/mL (high-dose group, H). The cells were cultured and then administered PPI as described above. At the endpoint of the experiment, 1×10^7 cells from the different groups were collected, incubated with 5 μL of Annexin V-fluorescein isothiocyanate (FITC) at room temperature in the dark for 15 min and then incubated with 5 μL of propidium iodide (PI). Finally, the stains were analyzed using a flow cytometer and the Pharmingen™ FITC Annexin V Apoptosis Detection Kit I according to the manufacturer's instructions (BD Biosciences, Franklin Lakes, USA).

Transcriptome analysis by RNA-seq

Hep3B 2.1–7 cells (1×10^8) from the different treatment groups and control were collected. The transcriptome analysis by RNA-seq was conducted according to our previous study [20, 21]. TRIzol reagent (R0016, Beyotime, Beijing, China) was used to extract the total RNA, which was then used to prepare the RNA-seq transcriptome library using the TruSeqTM RNA sample preparation Kit (Illumina, CA, USA). The Illumina NovaSeq 6000 platform (Illumina, San Diego, California) was used to process the short-sequenced fragments.

Western blotting

The total protein of the cells in the different groups was extracted using a protein extraction kit and the protein concentration estimated by the bicinchoninic acid (BCA) method (Biorigin, Beijing, China). SDS-PAGE (Millipore, Darmstadt, Germany) was used to separate the proteins,

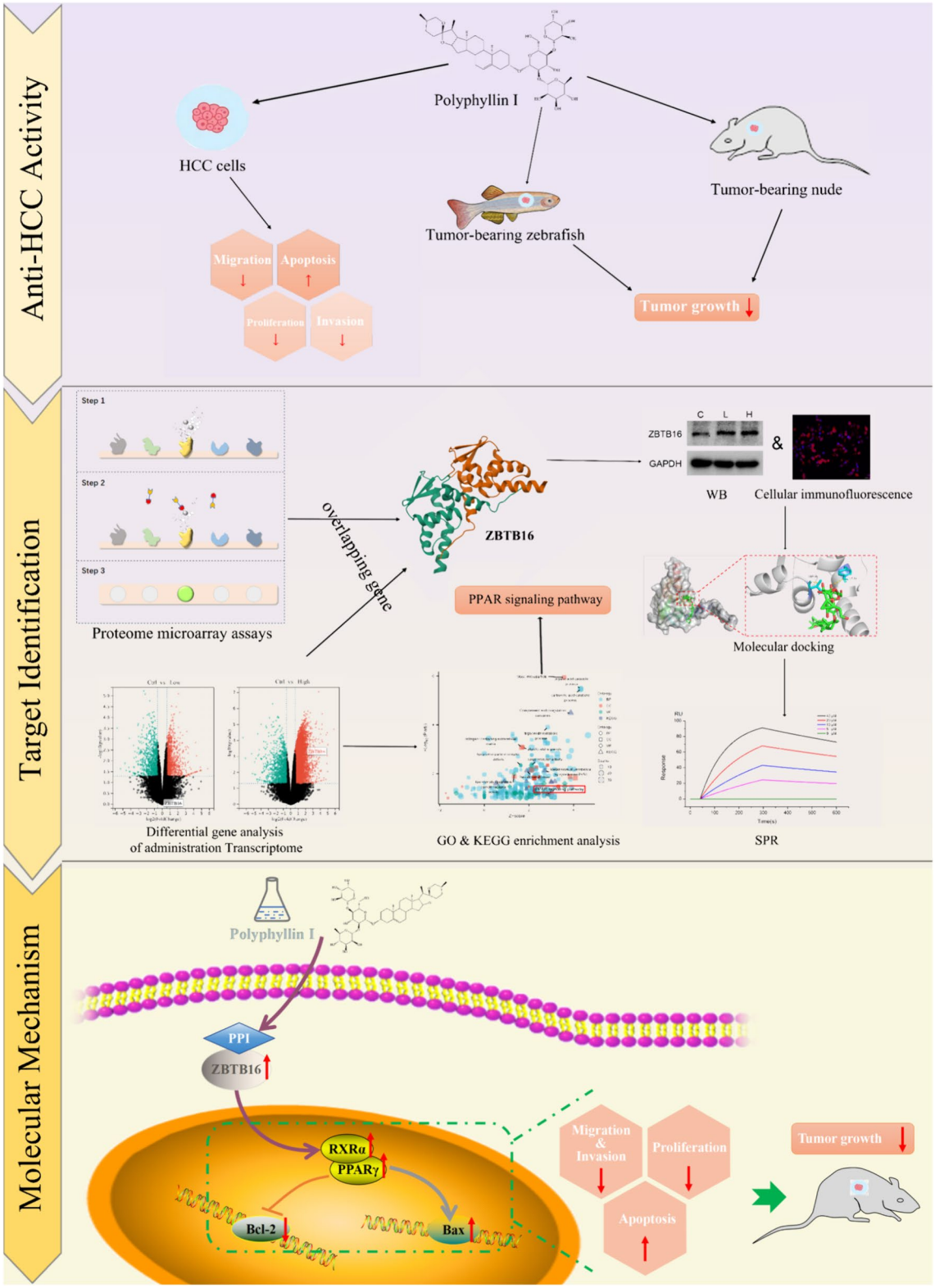

Fig. 1 Workflow of the current study

which were then transferred electrophoretically to a polyvinylidene difluoride membrane, blocked in 5% milk/Tris-buffered saline/Tween buffer and incubated overnight at 4 ℃ with the primary antibody. The following primary antibodies were used against GAPDH (Proteintech, Wuhan, China; Cat No. 60004-1-Ig, Lot #10028230, 1:1000), Caspase 3 (Proteintech, Cat No. 19677-1-AP, Lot #10018674, 1:1000), cleaved Caspase 3 (Affinity, Jiangsu, China; Cat No. AF7022, Lot #15z0096, 1:1000), ZBTB16 (Santa Cruz, CA, USA; Cat No. sc-28319, Lot #I1022, 1:500), PPARγ (Affinity, Cat No. AF6284, Lot #58o2063, 1:1000), RXRα (Affinity, Cat No. DF8459, Lot #00094775, 1:1000), Bcl2 (Affinity, Cat No. AF6139, Lot #11o9905, 1:1000), and Bax (Affinity, Cat No. AF0120, Lot #44q6915, 1:1000). The membranes were then incubated at room temperature for 90 min with the secondary antibodies (HRP conjugated anti-rabbit or anti-mouse IgG). Finally, the result of Western blotting was visualized using the ChemiDocTM MP Imaging System (Bio-Rad, State, USA; 734BR2920, USA) and analyzed using Image J software (NIH, Bethesda, MD, USA).

Xenograft tumor assay on zebrafish

The zebrafish embryos were obtained from spawning adults (5–8 months old) and raised at 28.5 °C in zebrafish embryo culture medium until 48 h after fertilization (hpf, hours after fertilization). The healthy zebrafish larvae were selected and microinjected with Hep3B 2.1–7 cells stained with CM-Dil (Beyotime, city, China) and then divided randomly into model, experimental, and control groups. After 24 h, the culture medium of the experimental groups was replaced with a culture medium containing different concentrations of PPI (low-dose group: 0.3 μg/mL, high-dose group: 0.6 μg/mL). An aliquot of 100 ng/ml of sorafenib (MCE, Shanghai, China) was added to the positive group [22, 23]. After 48 h, images were obtained using a Zeiss Axio Zoom V16 stereo fluorescent dissecting microscope (Carl Zeiss, Jena, Germany), and the fluorescence integrated density was calculated by Image J.

Proteome microarray assays

Arrayit HuProt™ 20 K human proteome microarrays (CDI Laboratories, MD, USA) were used and the experiment conducted according to the operating standard for chip detection. The microarrays were incubated with 40 mM biotinylated-PPI or free-biotin for 1 h at room temperature. After washing, 30 mL of Cy5 Streptavidin solution (1:100, Sigma-Aldrich, MO, USA) was added. The data were obtained by Genepix 4000B (Axon Instruments, Sunnyvale, CA, USA) and analyzed by GenePixTM Pro 6.0.

Surface plasmon resonance (SPR) analysis

The binding affinity of PPI to recombinant human ZBTB16 was determined at 22 °C using OpenSPR™ (manufacturer, city/state, country). Briefly, ZBTB16 proteins in PBS were immobilized on the sensor after activation by 200 μL EDC/NHS (1:1) in a water solution. Different concentrations of PPI were prepared in a running buffer (1% DMSO + HEPES). The binding time was 240 s, the dissociation time was 400 s, and the flow rate was 20 mL/min. The data were analyzed using TraceDrawer (Ridgeview Instruments ab, Vänge, Sweden).

Transfection of plasmids and small-interfering RNA

The siRNA oligonucleotides of ZBTB16 and Flag-tagged ZBTB16 plasmids were obtained from Jingmiga Technology Co. Ltd (Beijing, China). The Hep3B 2.1–7 cells were cultured to about 50% confluence before transfection. The siRNA and plasmids dissolved in an appropriate volume of MEM without the serum and antibiotics were incubated with appropriate transfection reagent and added to the cultured cells for 6 h according to the manufacturer's instructions. The medium was then changed to MEM containing 10% FBS and antibiotics. At the end of the experiments, the cell samples were collected for further analysis.

Mouse tumor xenograft studies

Specific pathogen-free (SPF) BALB/c nude mice (4–6 weeks old) were purchased from Beijing SiPeiFu Biotechnology Co., Ltd., and housed and fed in an SPF animal laboratory. The animal experiment was approved by the Animal Ethics Committee of Beijing University of Traditional Chinese Medicine (Animal Protocol No. BUCM-4-2021032003-1091). After a week of adaptive feeding, the mice were injected subcutaneously with cells (1×10^7 in 100 μL of PBS) and then randomized into treatment and control groups (eight mice per group), until the tumors reached a volume of 50 mm^3. Mice in the experimental groups were treated with 4 mg/kg (L) or 8 mg/kg (H) of PPI [24, 25] and the positive and model group with sorafenib (30 mg/kg) [17] or PBS, respectively. Each mouse was injected twice a week during the trial. The tumor size and body weight were monitored 2 or 3 times per week. The mice were anesthetized using isofluorane gas, followed by collection of the tumor xenografts, main organs, and blood samples.

Statistical analysis

All the statistical analyses were performed using GraphPad Prism 8.0 software. The results were expressed as mean ± SD based on a minimum of three independent repeated experiments. Dead animals were eliminated

from the data analysis. Comparison between the two groups was conducted using Student's t-test, while multiple group comparisons were conducted using one-way ANOVA. A p value < 0.05 indicated a statistically significant difference.

Results

PPI exerts anticancer activity in vivo *and* in vitro

To assess the antiproliferative function of PPI on HCC, the Hep3B 2.1–7 and SK-HEP-1 cell lines were treated with different concentrations of PPI. As shown in Fig. 2A–C, PPI markedly inhibited cell viability and colony formation ability in a concentration-dependent manner, especially in Hep3B cells (IC_{50} of Hep3B was 2.412 μg/mL and SK-Hep-1 was 5.059 μg/mL). Furthermore, wound healing and transwell invasion assays were performed to assess the effects of PPI on the migration and invasion of Hep3B cells, respectively. The results showed that PPI caused a significant decline in the migration of Hep3B cells and prevented the invasion of Hep3B cells in a concentration-dependent way (Fig. 2D–G). The flow cytometry results indicated that PPI also induced apoptosis in a concentration-dependent way (Fig. 2H), a finding that was confirmed by an elevated expression of cleaved caspase 3 (Fig. 2I, J). Similarly, PPI treatment suppressed tumor growth in the xenograft tumors of Hep3B cells in the zebrafish (Fig. 2K, L).

ZBTB16 was identified as a direct target of PPI

To investigate the potential action target of PPI in HCC, we labeled PPI with biotin and a fluorescent probe, and then performed a HuProt™20 K proteome microarray chip to detect the protein binding target to PPI. A total of 602 proteins showed significant specific interaction with PPI on the chip (Fig. 3A, B) that might have contributed to its biological anti-cancer activity. These 602 proteins were significantly enriched in GO entries such as the cytosol (Fig. 3C) and signaling pathways such as metabolic pathways (Fig. 3D).

To accurately identify potential targets of PPI, we conducted a series of analytical steps. Initially, we performed a differential gene analysis on the LIHC cohort from the TCGA database to identify significant gene expression differences between tumor and normal tissues (Figure S1A). Subsequently, we compared the transcriptomic data of HCC cells with and without PPI treatment to screen for genes whose expression significantly changed after the action of PPI (Figure S1B). We then intersected these two sets of differential genes with the potential binding target proteins of PPI predicted by chip technology, thereby identifying 30 potential targets at the center of the intersection (Figure S1C). Furthermore, we conducted Kaplan-Meier survival analysis on these genes and used WB technology to test whether the protein expression levels of genes with potential prognostic value for HCC patients changed with the dosage of PPI (Figure S1D). After this series of comprehensive analyses, we ultimately selected ZBTB16 as a candidate for further research because it not only showed significant prognostic relevance among all potential targets but also had a clear association with the action of PPI.

As show in Fig. 3E, the original signal intensity of the ZBTB16 protein on the PPI-chip was significantly higher than that on the biotin chip, indicating binding of PPI to ZBTB16 in HCC cells. Furthermore, the results of Western blotting and the cellular immunofluorescence assays indicated that PPI may potentially mediate its activities by binding to ZBTB16 proteins (Fig. 3F–H). SPR was then performed with the results demonstrating a high affinity between the recombinant human (rh) ZBTB16 protein and PPI, with a dissociation constant (K_D) of 5.5 μM (Fig. 3I). This finding was consistent with the results of molecular docking that showed the binding energy of the two was -10.4 cal/mol, indicating that PPI may interact with THR-55 and TYR-86 of ZBTB16 (Fig. 3J).

Correlation between ZBTB16 and HCC

To validate that ZBTB16 was a potential therapeutic target for HCC, we first compared the expression levels of ZBTB16 mRNA in HCC tissue and normal tissue in the TCGA and GTEx datasets. This showed that compared with normal tissue, the mRNA expression level of ZBTB16 in tumor samples was downregulated significantly (Fig. 4A). K-M survival analysis demonstrated that the expression of ZBTB16 was related closely to overall survival (OS) of the HCC patients, with high expression indicating better survival (Fig. 4B), especially in patients with stages III- IV cancers (Fig. 4C). The area under the

(See figure on next page.)

Fig. 2 PPI has anticancer activity in vivo and in vitro. **A** CCK8 assay of Hep3B2.1–7 and SK-HEP-1 cells treated with PPI (n = 3). **B**, **C** Colony formation assay of HCC cells treated with PPI (n = 3; L, 2.5 μg/mL PPI; H, 5 μg/mL PPI). **D**, **E** Wound healing assay of HCC cells treated with PPI (n = 3; L, 2.5 μg/mL PPI; H, 5 μg/mL PPI). **F**, **G** Transwell assay of HCC cells treated with PPI (n = 3; L; 2.5 μg/mL PPI; H, 5 μg/mL PPI). **H** Annexin V–FITC dual staining assay of HCC cells treated with PPI (n = 3; L, 2.5 μg/mL PPI; H, 5 μg/mL PPI). **I**, **J** Change in cleaved caspase 3 in HCC cells treated with PPI (n = 3; L, 2.5 μg/mL PPI; H, 5 μg/mL PPI). **K**, **L** PPI significantly inhibited the tumor growth of zebrafish xenograft models injected with Hep3B cells (n = 6; Positive control, 100 ng/mL sorafenib; L, 0.3 μg/mL PPI; H, 0.6 μg/mL PPI). (* $p < 0.05$, ** $p < 0.01$, *** $p < 0.001$)

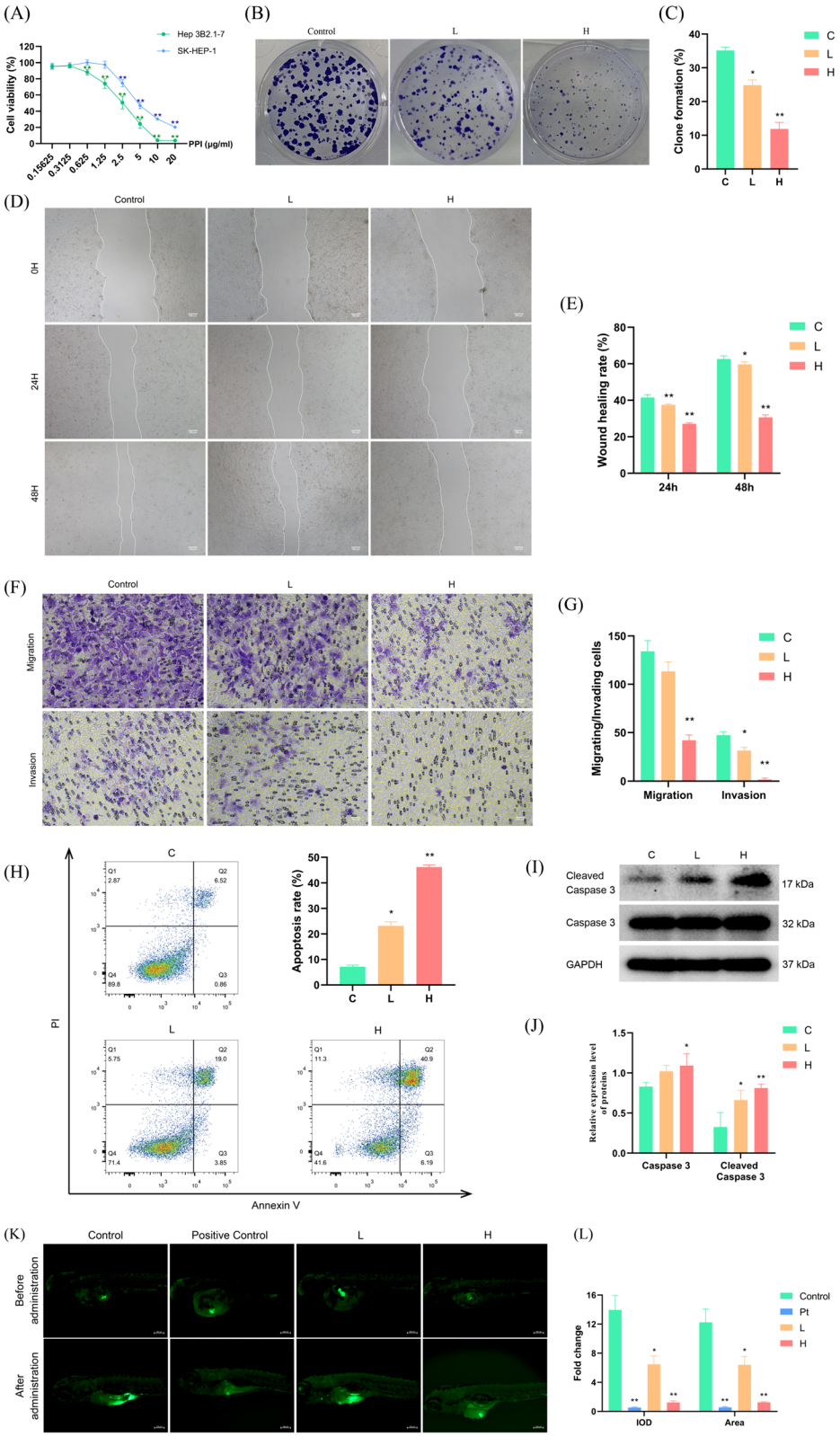

Fig. 2 (See legend on previous page.)

curve (AUC) of the diagnostic receiver operating characteristic (ROC) of ZBTB16 in HCC was 0.694 (95% CI, 0.648–0.741), indicating a good diagnostic value for HCC (Fig. 4D). Comparison of the composition of HCC patients in the high- and low-ZBTB16 groups showed that the proportion of patients with stage III-IV and grade 3–4 in the low group was higher than that in the high group (Fig. 4E, F). The correlation analysis between ZBTB16 and the clinical variables revealed a strong correlation between its expression and histological grade, gender, and alpha-fetoprotein (AFP) level (Fig. 4G, I), but no correlation with pathological grade (Fig. 4J). To further investigate the functional pathway of ZBTB16 regulation in HCC, we conducted differential gene analysis (GSEA) based on logFC of ZBTB16 high and low group differential genes. It was found that the PPAR signaling pathway was activated significantly in the high group (Fig. 4K). The correlation scatter plot also showed that the expression of ZBTB16 correlated negatively with the expression of cell proliferation-related genes (including Ki67 and PCNA) and HCC diagnostic markers (including GPC3 [26], OPN [27], and MMP1 [28]) (Fig. 4M–Q).

ZBTB16 inhibits HCC cell metastasis and growth in vitro

To investigate the function of ZBTB16 in HCC, we constructed knockdown and overexpression cell lines (Fig. 5A–D). The wound healing results showed that ZBTB16 knockdown significantly increased the migration activity of Hep3B2.1–7 cells in vitro. In contrast, ZBTB16 overexpression inhibited the migration of Hep3B2.1–7 cells (Fig. 5E, F). Similar results were observed in the transwell assay based on the characteristics of migration and invasion ability (Fig. 5G, I) of Hep3B2.1–7 cells (Fig. 5J, K). In addition, the inhibitory effect of ZBTB16 on the proliferation of Hep3B2.1–7 cells was confirmed by the results of the plate cloning experiment.

PPI inhibits HCC by targeting ZBTB16

To further confirm the important role of ZBTB16 in the anticancer activity of PPI, rescue experiments related to ZBTB16 were designed based on the inhibition of PPI in HCC cells. The results of the CCK8 assay showed that at the same dosage, the anti-proliferation effect of PPI on cells with ZBTB16 overexpression was enhanced significantly, while ZBTB16 knockout improved the inhibition of PPI in cells (Fig. 6A). Similar results of cell apoptosis were observed. As shown in Fig. 6B–D, ZBTB16 knockdown significantly abolished the effect of PPI-induced cell apoptosis. In contrast, cell apoptosis of the ZBTB16 overexpressing cell line treated with PPI was significantly higher than that of the PPI group, indicating that ZBTB16 had a key contribution in the anti-cancer effects of PPI.

Transcriptome analysis revealed the involvement of the PPAR signaling pathway in the anticancer activity of PPI

To determine the molecular mechanism associated with the anticancer activity of PPI, RNA sequencing of Hep3B cells was conducted. A principal component analysis (PCA) was conducted to detect the clustering trend in the multidimensional data, with the results indicating a distinct segregation between the low and high-PPI and control groups. Compared to the control group, there was a shift in principal component 1 (PC1) and PC2 in PPI (Fig. 7A). Differential gene analysis identified 1032 and 3950 genes as significantly differentially expressed genes (DEGs) in the low and high groups, respectively ($|\ \log FC\ | \geq 1$, $p < 0.05$) (Fig. 7B, C). ZBTB16 was upregulated significantly in the high group (Fig. 7C). To obtain an insight into the global patterns of the effects of DEGs on biological processes, we performed GO and KEGG analyses. Briefly, the results showed that DEGs in both the high and low groups were enriched significantly in the PPAR signaling pathway ($p < 0.05$) (Fig. 7D, E). To gain a more comprehensive understanding of the pathways altered in response to PPI, a heatmap of Gene Set Variation Analysis (GSVA) was generated from the transcriptome data. As shown in Fig. 7F, PPI may exert its anticancer activity by activating the PPAR signaling pathway and inducing apoptosis. Through the protein–protein interaction network, it was found that in the PPAR signaling pathway, ZBTB16 only interacts with RXRα, which regulates cell apoptosis by forming heterodimers with PPARγ (Fig. 7G) [29–31]. Based on the TCGA-LIHC dataset, we also showed that ZBTB16 was significantly

(See figure on next page.)

Fig. 3 ZBTB16 was identified as a direct target of PPI. **A** HuProt™20 K Proteome microarray chip indicating the protein targets binding to PPI. The yellow arrow points to the location of the ZBTB16 protein. **B** Venn diagram of the protein targets binding to biotin and PPI. **C**, **D** GO and KEGG enrichment analysis of the specific binding proteins of PPI. **E** The signal intensity of the ZBTB16 protein in the HuProt™20 K proteome microarray chip. **F**–**H** Changes in the expression of the ZBTB16 protein in HCC cells treated with PPI (n = 3; L, 2.5 μg/mL PPI; H, 5 μg/mL PPI). **I** SPR analysis of binding affinity between PPI and the ZBTB16 protein. **J** Molecular docking analysis of PPI binding to the ZBTB16 protein to predict the binding site. (* $p < 0.05$, ** $p < 0.01$, *** $p < 0.001$)

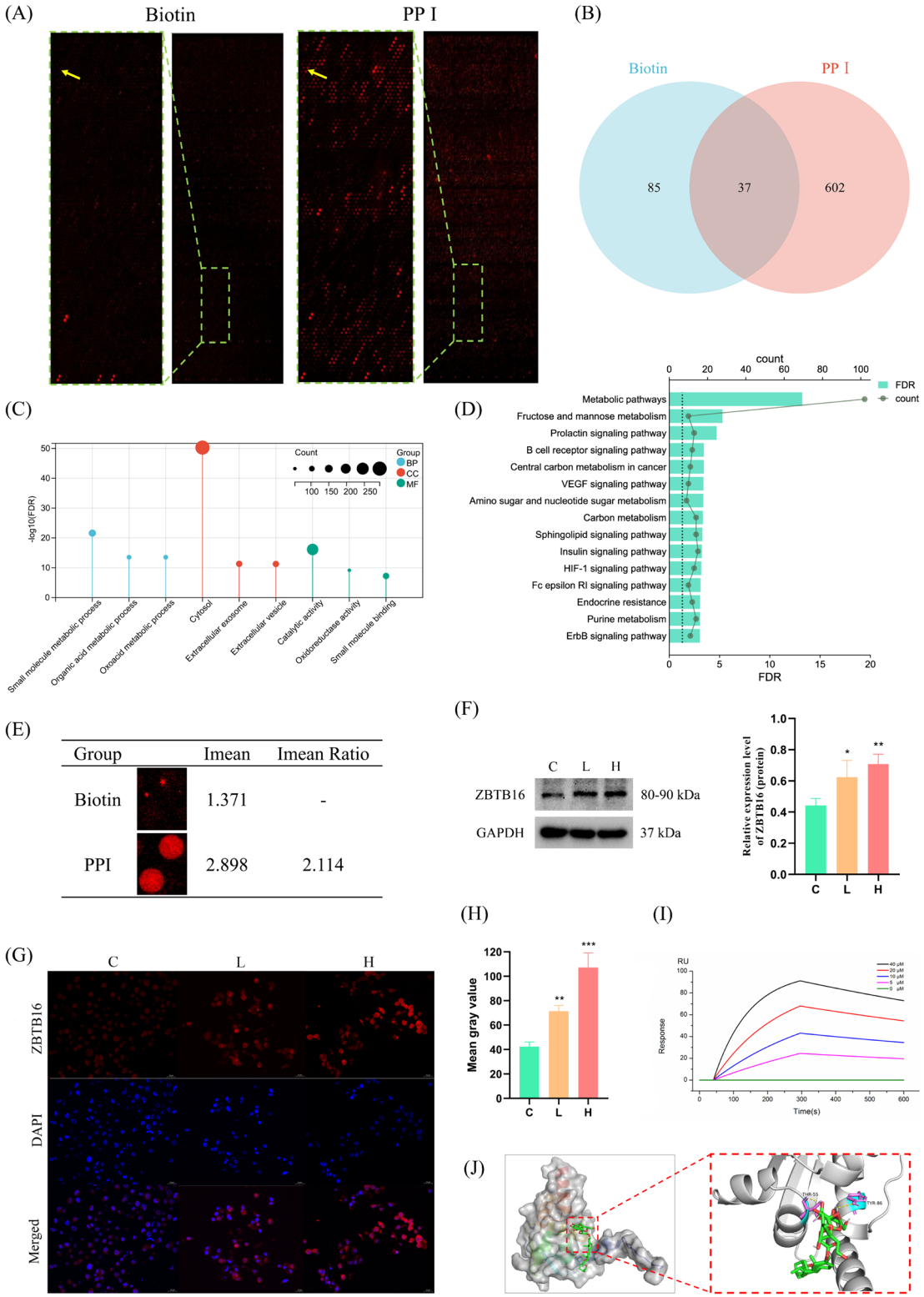

Fig. 3 (See legend on previous page.)

and positively correlated with RXRα, but not with PPARγ (Fig. 7H). The WB results demonstrated that PPI activated the PPAR signaling pathway by increasing RXRα and PPARγ significantly, and upregulated Bax but decreased Bcl-2 protein ($p < 0.05$), leading to apoptosis in Hep3B cells (Fig. 7I, J).

PPI inhibits the growth of HCC in vivo *without causing significant host toxicity*

To determine whether PPI inhibited tumor growth in vivo, we examined it effect on Hep3B-derived tumors in BALB/c mice (Fig. 8A). Following an intraperitoneal injection of PPI (4 or 8 mg/kg) once daily for 28 d, PPI significantly prevented body weight loss induced by tumors (Fig. 8B). Furthermore, consistent with our in vitro findings, PPI treatment led to a substantial reduction in tumor volume and tumor weight in the xenograft model mice compared with those of the control group (Fig. 8C–E). Pathological examination by HE staining showed that the xenograft tumor cells were packed loosely with small nuclei compared with that observed in the control group (Fig. 8F). In the IHC assays, PPI enhanced ZBTB16 but strongly suppressed the Ki-67, indicating that PPI contributed to the major effect on tumor cell survival (Fig. 8F–H). Meanwhile, PPI induced the up-regulation of TUNEL-positive cells, confirming PPI triggering significant apoptosis in the tumor cells (Fig. 8F–I). Additionally, to evaluate the side effects of PPI, the histology of the liver and kidney were monitored and recorded. Our results showed no observable damage to the liver and kidney in PPI-treated mice (Fig. 8F). This finding was confirmed by histological analysis of the major organs, which showed no observable difference between the control and treated groups.

We next examined the effects of PPI on signaling activity in the transplanted tumors. In line with the in vitro results, ZBTB16 and PPARγ, RXRα protein levels were both increased (Fig. 8J, K), which confirmed that PPI effectively inhibits tumor growth by targeting ZBTB16 to activate the PPARγ/RXRα signaling pathway.

Discussion

HCC is one of the most common malignant tumors in clinical practice and is associated with an extremely high incidence and mortality rate [3]. Therefore, the development of effective therapeutic agents for the treatment of HCC has always been a promising strategy. TCM has demonstrated substantial clinical benefits, playing a crucial role in the prevention and management of liver precancerous conditions, serving as an adjuvant therapy for HCC, and preventing post-surgical recurrence [32–35]. For example, clinical studies have confirmed the efficacy of Huaier Granules when used adjunctively after surgical resection and in combination with TACE, significantly reducing HCC recurrence rates [33, 34]. Similarly, numerous studies have shown that PPI has promising potential for treating various cancers [36–39]. However, the mechanism of its role for treating and slowing down the progression of HCC remains elusive and there remains an urgent need for further in-depth research.

The present study demonstrated that PPI inhibited the progression of HCC in vivo and in vitro by inhibiting proliferation, inducing apoptosis, and preventing migration and invasion. Furthermore, PPI showed no apparent toxicity to the liver and kidney of tumor-bearing mice at effective doses, preliminarily indicating its safety. Notably, the clinical use of PPI is currently problematic because of its potential adverse effects [40–43]. Although an 8 mg/kg dose in our in vivo experiments did not result in toxicity, a recent study reported that higher doses may produce adverse effects [43].

ZBTB16 was identified as the critical binding target protein of PPI against HCC in this study. It has been identified as a tumor suppressor gene of HCC, breast cancer, gastric cancer, and prostate cancer [16, 44–46], in which the mechanism of ZBTB16-mediated tumor inhibition was mainly related to cell cycle arrest, apoptosis induction, and EMT inhibition [14, 44, 47]. Our results showed that ZBTB16 knockdown promoted HCC cell proliferation in vitro and ZBTB16 overexpression

(See figure on next page.)

Fig. 4 ZBTB16 is inhibited significantly in HCC and is associated with an improved prognosis in patients with the malignancy. **A** ZBTB16 mRNA expression is downregulated in HCC tissues compared with that in the normal tissue groups of the TCGA and GTEx datasets. **B** Kaplan–Meier survival analysis on the association between ZBTB16 expression and overall survival of patients. **C** Kaplan–Meier survival analysis on the association between ZBTB16 expression and overall survival of patients with stage III-IV HCC in the TCGA-LIHC dataset. **D** Diagnostic receiver operating characteristics curves of ZBTB16 in HCC. **E** Composition of the pathologic stage of the ZBTB16-high (n = 173) and -low groups (n = 173) in the TCGA-LIHC dataset. **F** Composition of the histologic grade of the high-ZBTB16 (n = 173) and low-ZBTB16 groups (n = 173) in the TCGA-LIHC dataset. **G**–**J** Comparison of ZBTB16 mRNA expression in the different HCC clinical groups. **K** The GSEA results indicated that the PPAR signaling pathway was enriched significantly in the high-ZBTB16 group. **L**–**P** Correlation analysis of ZBTB16 and mRNA expression levels in the indicated genes in the TCGA-LIHC dataset. (* $p < 0.05$, ** $p < 0.01$, *** $p < 0.001$)

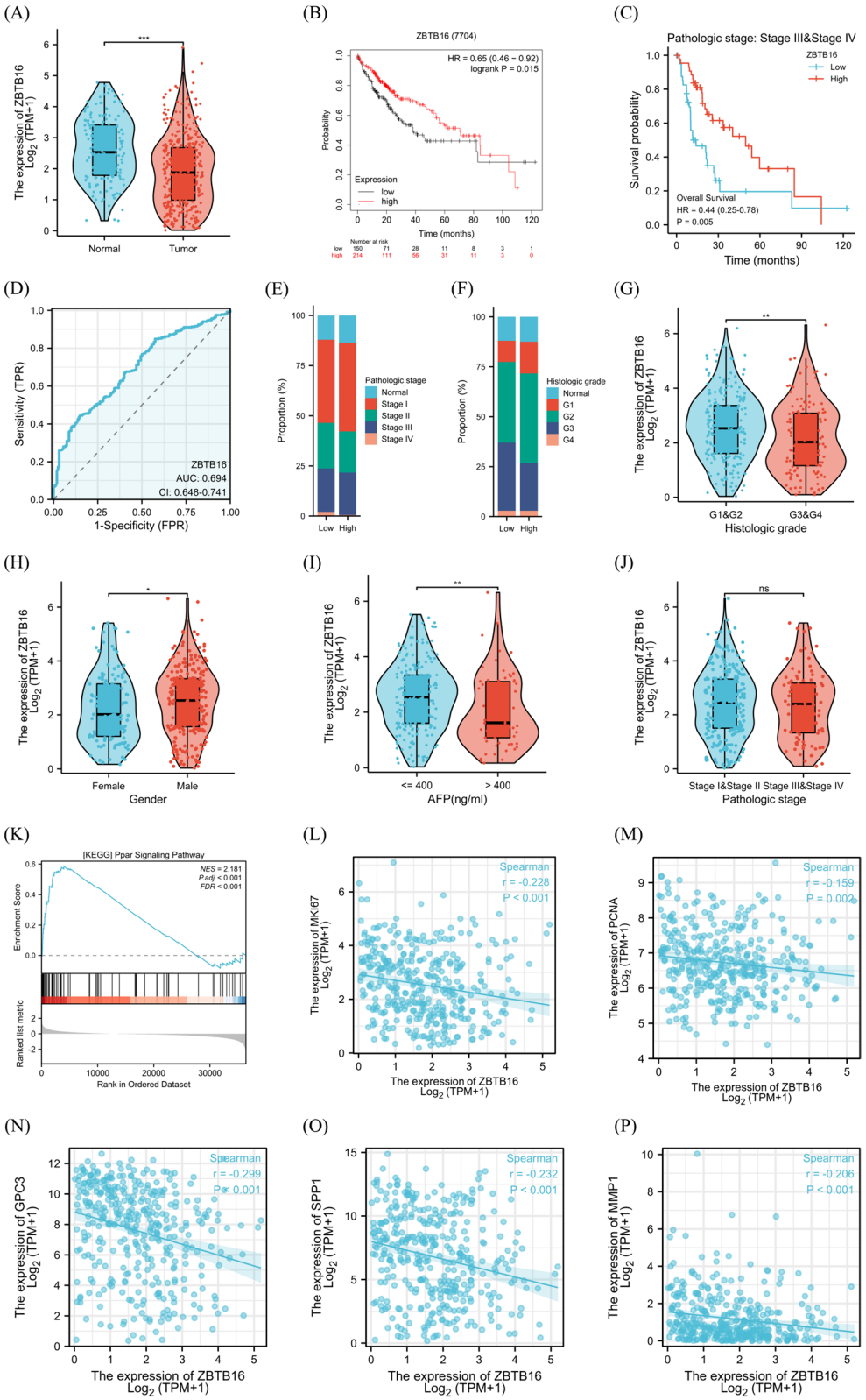

Fig. 4 (See legend on previous page.)

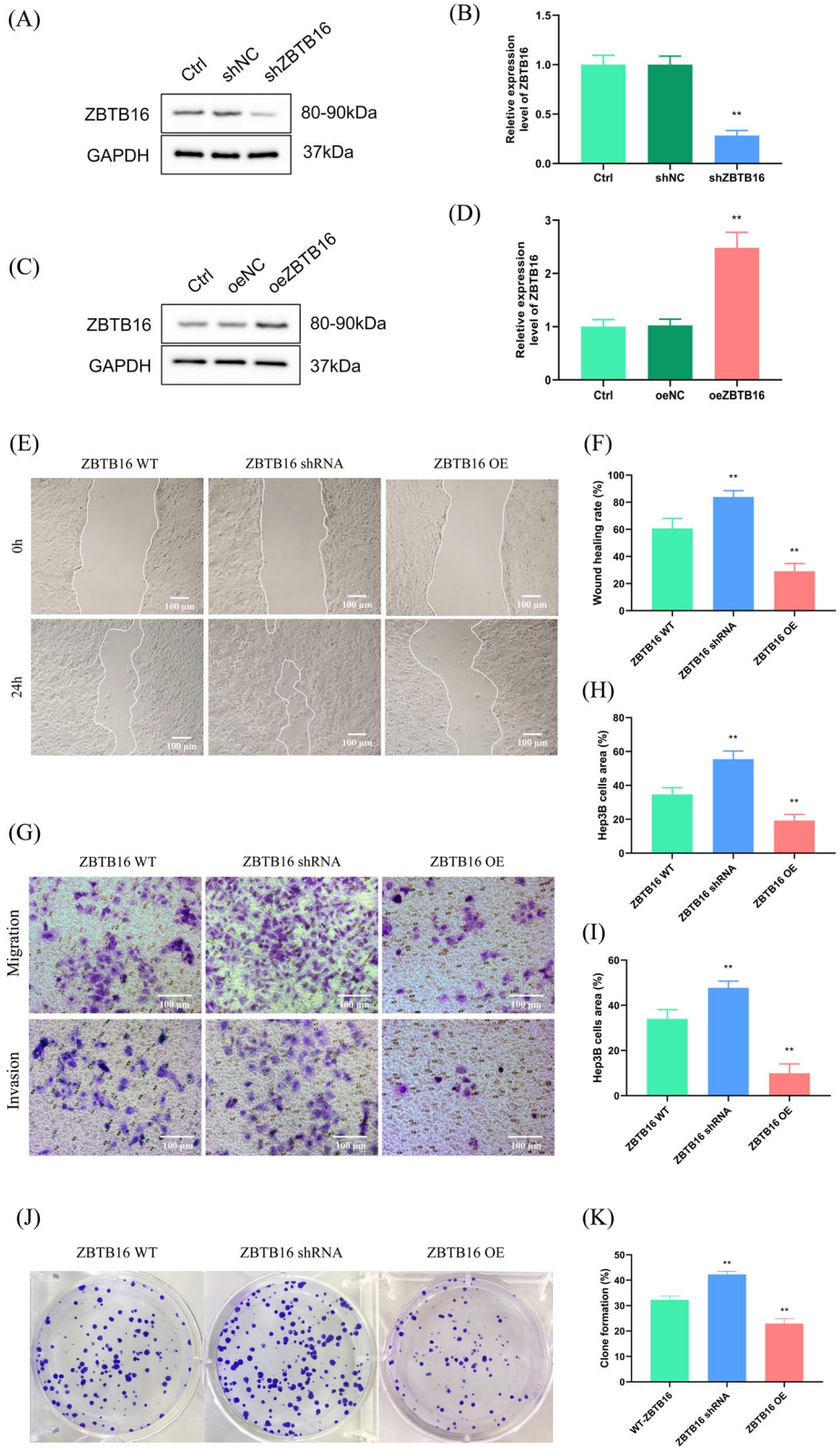

Fig. 5 ZBTB16 inhibits cancer cell metastasis and growth in vitro. **A**–**D** ZBTB16 knockdown and overexpressing cell lines were constructed (n = 3). **E**, **F** Wound healing assay using ZBTB16 knockdown and overexpression cell lines (n = 3). **G**–**I** Migration and invasion ability in ZBTB16 knockdown and overexpression cell lines (n = 3). **J**, **K** Cloning formation assay in ZBTB16 knockdown and overexpression cell lines (n = 3). (* $p < 0.05$ and ** $p < 0.01$)

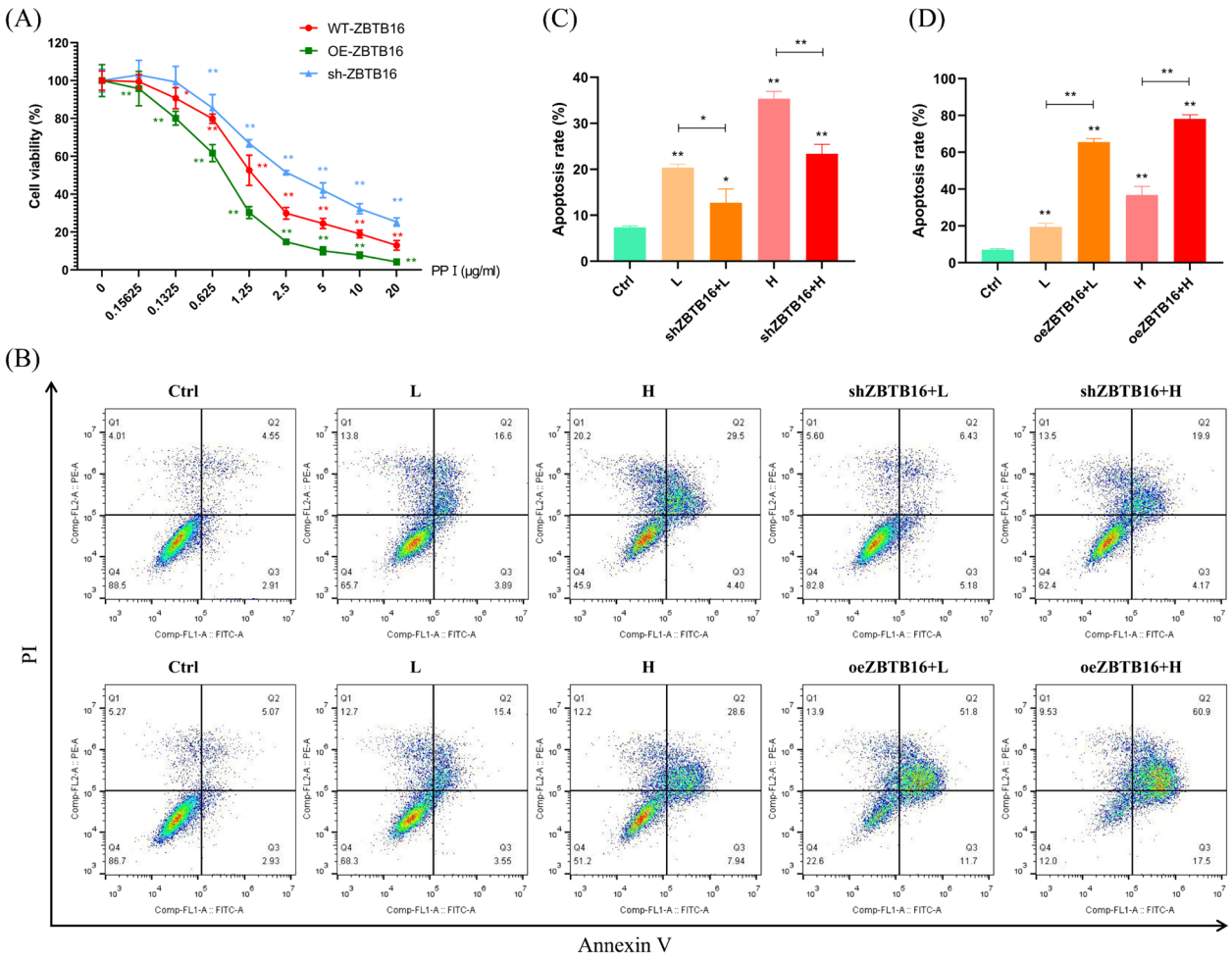

Fig. 6 PPI inhibits HCC by targeting ZBTB16. **A** CCK8 assay of ZBTB16 knockdown and overexpression cell lines with PPI (n = 3). **B**–**D** Annexin V–FITC dual staining assay of ZBTB16 knockdown and overexpression cell lines with PPI (n = 3). (L, 2.5 μg/mL PPI; H, 5 μg/mL PPI) (* $p < 0.01$, ** $p < 0.001$)

(See figure on next page.)

Fig. 7 Transcriptome analysis showing the involvement of the PPAR signaling pathway in the anticancer activity of PPI. **A** PCA of transcriptomes with or without different concentrations of PPI represented in a two-dimensional space. **B**, **C** Volcano plot of differential genes in HCC cells induced by low- and high-dose PPI treatment. **D** Bubble plots for the GO and KEGG enrichment analysis of differentially expressed genes induced by low-dose PPI. **E** Bubble plots for the GO and KEGG enrichment analysis of differentially expressed genes induced by high-dose PPI. **F** Heat map showing the GSVA enrichment score for apoptosis and the PPAR signaling pathway in the transcriptome of HCC cells treated with PPI. **G** PPI network of the ZBTB16 and PPAR signaling pathways. **H** Heatmap showing the correlation between the mRNA expression level of ZBTB16, PPARγ, and RXRα. **I**, **J** The regulatory effect of PPI on the PPAR signaling pathway in HCC cells (n = 3; L, 2.5 μg/mL PPI; H, 5 μg/mL PPI). (* $p < 0.05$, ** $p < 0.01$, *** $p < 0.001$)

blocked metastasis of HCC cell, which are consistent with the conclusions of existing studies. In addition, we also found that the abnormal down-regulation of ZBTB16 in HCC was strongly associated with poor prognosis, higher histological grade, and higher levels of APF. Thus, the ZBTB16 may serve as a promising biomarker and therapeutic target for the treatment of HCC patients and selective promotion of ZBTB16 remains an active area of drug development. PPI does represent a new lead compound for further design and discovery of ZBTB16 agonists. Attempts at modifying PPI to reduce its toxicity, controlled release, and using PPI format or in targeted/combinatorial therapies may help its clinical use.

To provide better insights into the full spectrum of the anti-HCC activity of PPI at the molecular level, a transcriptome in Hep3B cells was performed to confirm the

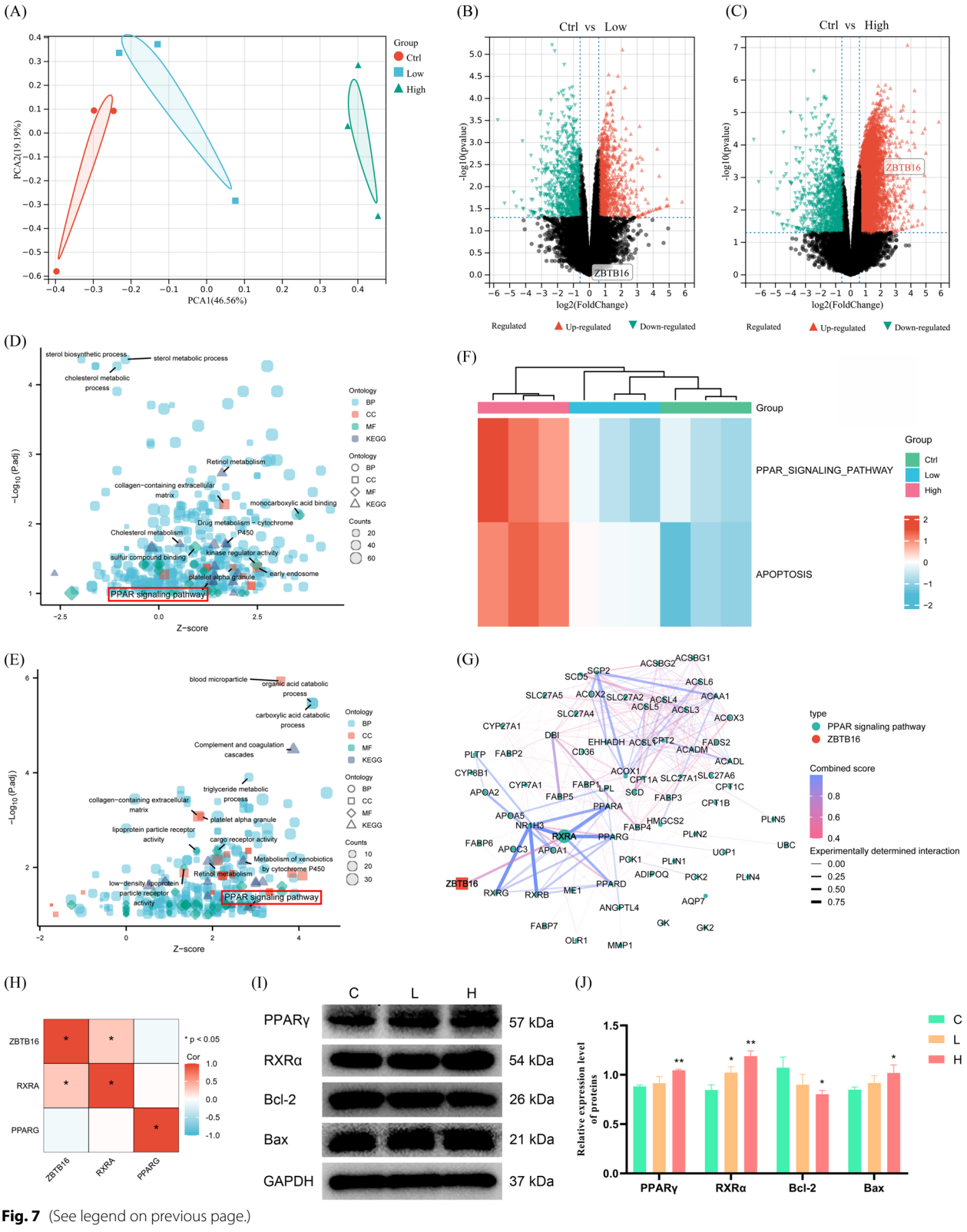

Fig. 7 (See legend on previous page.)

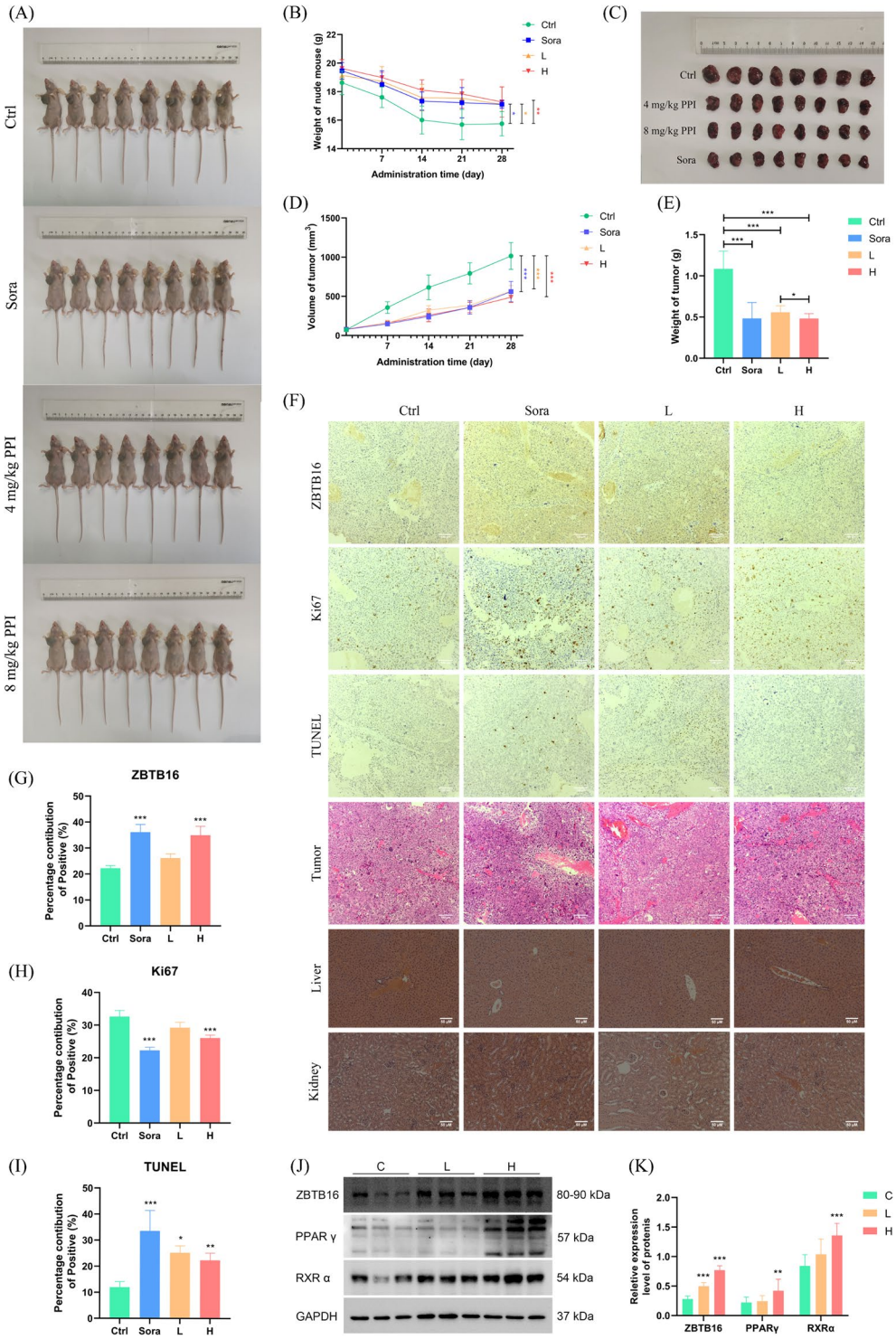

Fig. 8 PPI inhibits the growth of HCC in vivo without causing significant host toxicity. **A** Photos of nude mice in each group at the end of the experiment. **B** Graph showing the change in body weight of the nude mice in each group during administration of PPI. **C**–**E** PPI significantly inhibited tumor growth in the mouse xenograft models injected with Hep3B (n = 8). **F**–**I** Immunohistochemical and Tunel assay of tumor bodies and liver and kidney sections in the nude mice in each group. **J**, **K** PPI significantly activated the ZBTB16-mediated PPAR signaling pathway (n = 3). (C, control; Sora, 30 mg/kg sorafenib; L, 4 mg/kg PPI; H, 8 mg/kg PPI) (* $p < 0.05$, ** $p < 0.01$, *** $p < 0.001$)

key pathways involved in the response to the direct binding between the PPI and ZBTB16. The in-depth transcriptome analysis revealed that the inhibitory effects of ZBTB16 and PPI on HCC were involved in activating the PPAR signaling pathway. Besides, ZBTB16 was closely related to RXRα in the PPAR signaling pathway. It is reported that Peroxisome proliferator-activated receptor gamma (PPARγ) is mainly involved in the occurrence, progression and resistance development of HCC through regulating lipid metabolism [48–53], but its precise role remains controversial [54–56]. According to the experimental results in vivo and in vitro, we speculated that PPI promotes the combination of RXRα and PPARγ by targeting ZBTB16, leading to the inhibitory effect on the malignant phenotype of tumor cells. Moreover, combining ZBTB16 and PPARγ also played an important role in immunotherapy. It has been reported that activating the combination of the two would promote lipid biosynthesis, thereby improving the anti-tumor function of invariant natural killer T (iNKT) cells in the tumor microenvironment [57]. Briefly, ZBTB16 and RXRα/PPARγ pathway may be therapeutic for HCC.

It is important to note that ZBTB16 is not the only target of PPI, as PPI appears to interact with multiple target proteins. For example, our protein arrays showed that PPI potentially interacted with the shock transducer and activator of transcription 3 (STAT3) [58–60], mitogen-activated protein kinase 3 (MAPK3) [61–63], the HECT domain, and the Ankyrin Repeat Containing E3 Ubiquitin Protein Ligase 1 (HACE1) [64, 65], all of which are linked to cancer pathogenesis. Therefore, further studies are certainly warranted to determine the contribution of these potential PPI targets in HCC and other cancers.

Conclusion

Briefly, our study indicated that ZBTB16 is a promising drug target for PPI against HCC. This supports the development of PPI as a promising therapeutic agent for regulating the ZBTB16/PPARγ/RXRα signaling axis, an action that has great potential to provide important clinical benefits.

Abbreviations

AFP	Alpha-fetoprotein
APL	Acute promyelocytic leukemia
AUC	Area under the curve
BCA	Bicinchoninic acid
BP	Biological process
CC	Cellular component
CCK8	Cell counting kit-8
DEGs	Differentially expressed genes
FBS	Fetal bovine serum
FC	Foldchange
GO	Gene ontology
GSEA	Gene set enrichment analysis
HACE1	HECT domain, and Ankyrin repeat containing E3 ubiquitin protein ligase 1
HCC	Hepatocellular carcinoma
IHC	Immunohistochemistry
KD	Dissociation constant
KEGG	Kyoto Encyclopedia of Genes and Genomes
LIHC	Liver hepatocellular carcinoma
MAPK3	Mitogen-activated protein kinase 3
MF	Molecular function
NC membranes	Nitrocellulose membranes
OS	Overall survival
P/S	Penicillin and streptomycin
PBS	Phosphate-Buffered Saline
PCA	Principal component analysis
PLZF	Promyelocytic leukemia zinc finger protein
PPI	Polyphyllin I
PPARγ	Peroxisome proliferator-activated receptor gamma
RARα	Retinoic acid receptor alpha
ROC	Receiver operating characteristic
RXRα	Retinoid X receptor alpha
SDS-PAGE	Sodium dodecyl sulfate–polyacrylamide gel electrophoresis
SPR	Surface plasmon resonance
STAT3	Shock transducer and activator of transcription 3
TCGA	The Cancer Genome Atlas Program
TCM	Traditional Chinese medicine
ZBTB16	Zinc finger and BTB domain-containing 16

Supplementary Information

The online version contains supplementary material available at https://doi.org/10.1186/s13020-024-00984-0.

Supplementary Material 1

Acknowledgements

We are grateful to the Beijing Key Laboratory of Traditional Chinese Medicine Quality Evaluation for providing experimental instruments and equipment. We thank the Beijing University of Chinese Medicine for providing the laboratory platform. We would like to express our gratitude to EditSprings (https://www.editsprings.cn) for the expert linguistic services provided.

Author contributions

Shan Lu: investigation, writing – original draft, data curation. Yijun Chen: investigation. Guo An: investigation. Xiaoyu Tao: investigation and data curation. Chuanqi Qiao: investigation. Meilin Chen: data curation. Jiaqi Li: data curation. Ruichao Lin: funding acquisition, writing—review & editing. Jiarui Wu: supervision, writing—review & editing. Chongjun Zhao: project administration, conceptualization, methodology, writing—review & editing. All authors read and approved the final manuscript. All authors read and approved the final manuscript.

Funding

This work was supported by a grant from the National Natural Science Foundation of China (NO. 82204753). The funder had no role in the study design, data collection, data analysis, interpretation, or writing of the report.

Availability of data and materials

The datasets used and/or analyzed during the current study are available from the corresponding author on reasonable request.

Declarations

Ethics approval and consent to participate

The experiment was in accordance with the Animal Management Rules of the Ministry of Science and Technology of the People's Republic of China for experimental care and use of animals and approved by the Animal Ethics Committee of Beijing University of Traditional Chinese Medicine. (Animal Protocol No. BUCM-4-2021032003-1091).

Consent for publication
Not applicable.

Competing interests
The authors declare that there are no competing interests.

Received: 4 June 2024 Accepted: 13 August 2024
Published online: 24 August 2024

References

1. Allemani C, Matsuda T, Di Carlo V, Harewood R, Matz M, Nikšić M, et al. Global surveillance of trends in cancer survival 2000–14 (CONCORD-3): analysis of individual records for 37 513 025 patients diagnosed with one of 18 cancers from 322 population-based registries in 71 countries. Lancet. 2018;391(10125):1023–75.
2. Li C, Lu X, Gao F, Lee E, Chan CWH. Development of a nurse-led decision counseling program for improving hepatocellular carcinoma screening: a typology-guided feasibility study. Asia Pac J Oncol Nurs. 2023;10(6):100215.
3. Sung H, Ferlay J, Siegel RL, Laversanne M, Soerjomataram I, Jemal A, et al. Global cancer statistics 2020: GLOBOCAN estimates of incidence and mortality worldwide for 36 cancers in 185 countries. CA Cancer J Clin. 2021;71(3):209–49.
4. Hassanipour S, Vali M, Gaffari-Fam S, Nikbakht HA, Abdzadeh E, Joukar F, et al. The survival rate of hepatocellular carcinoma in Asian countries: a systematic review and meta-analysis. Excli j. 2020;19:108–30.
5. Kloeckner R, Galle PR, Bruix J. Local and regional therapies for hepatocellular carcinoma. Hepatology. 2021;73(Suppl 1):137–49.
6. Zou H, Zhu CZ, Wang C, Wang ZS, Ma X, Han B, et al. Recurrence of barcelona clinic liver cancer stage a hepatocellular carcinoma after hepatectomy. Am J Med Sci. 2017;354(3):262–7.
7. Lu Y, Gao Y, Yang H, Hu Y, Li X. Nanomedicine-boosting icaritin-based immunotherapy of advanced hepatocellular carcinoma. Mil Med Res. 2022;9(1):69.
8. Yu Z, Guo J, Hu M, Gao Y, Huang L. Icaritin exacerbates mitophagy and synergizes with doxorubicin to induce immunogenic cell death in hepatocellular carcinoma. ACS Nano. 2020;14(4):4816–28.
9. Luo XY, Wu KM, He XX. Advances in drug development for hepatocellular carcinoma: clinical trials and potential therapeutic targets. J Exp Clin Cancer Res. 2021;40(1):172.
10. Dowse RT, Ireland RM. Variant ZBTB16-RARA translocation: morphological changes predict cytogenetic variants of APL. Blood. 2017;129(14):2038.
11. Xiao GQ, Priemer DS, Wei C, Aron M, Yang Q, Idrees MT. ZBTB16 is a sensitive and specific marker in detection of metastatic and extragonadal yolk sac tumour. Histopathology. 2017;71(4):562–9.
12. Vincent-Fabert C, Platet N, Vandevelde A, Poplineau M, Koubi M, Finetti P, et al. PLZF mutation alters mouse hematopoietic stem cell function and cell cycle progression. Blood. 2016;127(15):1881–5.
13. Poplineau M, Vernerey J, Platet N, N'Guyen L, Hérault L, Esposito M, et al. PLZF limits enhancer activity during hematopoietic progenitor aging. Nucleic Acids Res. 2019;47(9):4509–20.
14. Noh KH, Jeong AJ, Lee H, Lee SH, Yi E, Chang PS, et al. Crosstalk between prostate cancer cells and tumor-associated fibroblasts enhances the malignancy by inhibiting the tumor suppressor PLZF. Cancers. 2020. https://doi.org/10.3390/cancers12051083.
15. Hui AW, Lau HW, Cao CY, Zhou JW, Lai PB, Tsui SK. Downregulation of PLZF in human hepatocellular carcinoma and its clinical significance. Oncol Rep. 2015;33(1):397–402.
16. He J, Wu M, Xiong L, Gong Y, Yu R, Peng W, et al. BTB/POZ zinc finger protein ZBTB16 inhibits breast cancer proliferation and metastasis through upregulating ZBTB28 and antagonizing BCL6/ZBTB27. Clin Epigenetics. 2020;12(1):82.
17. Liao M, Du H, Wang B, Huang J, Huang D, Tong G. Anticancer effect of polyphyllin I in suppressing stem cell-like properties of hepatocellular carcinoma via the AKT/GSK-3β/β-catenin signaling pathway. Oxid Med Cell Longev. 2022;2022:4031008.
18. Luo Q, Yang D, Qi Q, Huang C, Chen B, Liu W, et al. Role of the death receptor and endoplasmic reticulum stress signaling pathways in Polyphyllin I-regulated apoptosis of human hepatocellular carcinoma HepG2 cells. Biomed Res Int. 2018;2018:5241941.
19. Zeng Y, Zhang Z, Wang W, You L, Dong X, Yin X, et al. Underlying mechanisms of apoptosis in HepG2 cells induced by Polyphyllin I through Fas death and mitochondrial pathways. Toxicol Mech Methods. 2020;30(6):397–406.
20. Huang Z, Wu C, Zhou W, Lu S, Tan Y, Wu Z, et al. Compound Kushen Injection inhibits epithelial-mesenchymal transition of gastric carcinoma by regulating VCAM1 induced by the TNF signaling pathway. Phytomedicine. 2023;118:154984.
21. Liu X, Bai M, Li H, Ye P, Duan X, Wu C, et al. Single-cell RNA-sequencing uncovers compound kushen injection synergistically improves the efficacy of chemotherapy by modulating the tumor environment of breast cancer. Front Immunol. 2022;13:965342.
22. Kološa K, Žegura B, Štampar M, Filipič M, Novak M. Adverse toxic effects of tyrosine kinase inhibitors on non-target zebrafish liver (ZFL) cells. Int J Mol Sci. 2023. https://doi.org/10.3390/ijms24043894.
23. Yao Y, Sun S, Wang J, Fei F, Dong Z, Ke AW, et al. Canonical Wnt signaling remodels lipid metabolism in zebrafish hepatocytes following ras oncogenic insult. Cancer Res. 2018;78(19):5548–60.
24. Li GB, Fu RQ, Shen HM, Zhou J, Hu XY, Liu YX, et al. Polyphyllin I induces mitophagic and apoptotic cell death in human breast cancer cells by increasing mitochondrial PINK1 levels. Oncotarget. 2017;8(6):10359–74.
25. Long J, Pi X. Polyphyllin I promoted melanoma cells autophagy and apoptosis via PI3K/Akt/mTOR signaling pathway. Biomed Res Int. 2020;2020:5149417.
26. Pang N, Shi J, Qin L, Chen A, Tang Y, Yang H, et al. IL-7 and CCL19-secreting CAR-T cell therapy for tumors with positive glypican-3 or mesothelin. J Hematol Oncol. 2021;14(1):118.
27. Zhu M, Zheng J, Wu F, Kang B, Liang J, Heskia F, et al. OPN is a promising serological biomarker for hepatocellular carcinoma diagnosis. J Med Virol. 2020. https://doi.org/10.1002/jmv.25704.
28. Yang L, Rong W, Xiao T, Zhang Y, Xu B, Liu Y, et al. Secretory/releasing proteome-based identification of plasma biomarkers in HBV-associated hepatocellular carcinoma. Sci China Life Sci. 2013;56(7):638–46.
29. He BC, Chen L, Zuo GW, Zhang W, Bi Y, Huang J, et al. Synergistic antitumor effect of the activated PPARgamma and retinoid receptors on human osteosarcoma. Clin Cancer Res. 2010;16(8):2235–45.
30. Shankaranarayanan P, Rossin A, Khanwalkar H, Alvarez S, Alvarez R, Jacobson A, et al. Growth factor-antagonized rexinoid apoptosis involves permissive PPARgamma/RXR heterodimers to activate the intrinsic death pathway by NO. Cancer Cell. 2009;16(3):220–31.
31. Yamazaki K, Shimizu M, Okuno M, Matsushima-Nishiwaki R, Kanemura N, Araki H, et al. Synergistic effects of RXR alpha and PPAR gamma ligands to inhibit growth in human colon cancer cells–phosphorylated RXR alpha is a critical target for colon cancer management. Gut. 2007;56(11):1557–63.
32. Yang T, Liao Y, Lyu W. Research on the application of traditional Chinese medicine in the prevention and treatment of liver precancerous lesions. Front Med Sci Res. 2023;5(9):24–31.
33. Wei L, Wang Z, Jing N, Lu Y, Yang J, Xiao H, et al. Frontier progress of the combination of modern medicine and traditional Chinese medicine in the treatment of hepatocellular carcinoma. Chin Med. 2022;17(1):90.
34. Peng Y, Wu X, Zhang Y, Yin Y, Chen X, Zheng D, et al. An overview of traditional Chinese medicine in the treatment after radical resection of hepatocellular carcinoma. J Hepatocell Carcinoma. 2023;10:2305–21.
35. Liao X, Bu Y, Jia Q. Traditional Chinese medicine as supportive care for the management of liver cancer: past, present, and future. Genes Dis. 2019;7(3):370–9.
36. He J, Yu S, Guo C, Tan L, Song X, Wang M, et al. Polyphyllin I induces autophagy and cell cycle arrest via inhibiting PDK1/Akt/mTOR signal and downregulating cyclin B1 in human gastric carcinoma HGC-27 cells. Biomed Pharmacother. 2019;117:109189.
37. Luo Q, Jia L, Huang C, Qi Q, Jahangir A, Xia Y, et al. Polyphyllin I promotes autophagic cell death and apoptosis of colon cancer cells via the ROS-inhibited AKT/mTOR pathway. Int J Mol Sci. 2022. https://doi.org/10.3390/ijms23169368.

38. Zheng F, Wang Y, Zhang Q, Chen Q, Liang CL, Liu H, et al. Polyphyllin I suppresses the gastric cancer growth by promoting cancer cell ferroptosis. Front Pharmacol. 2023;14:1145407.
39. Tian Y, Gong GY, Ma LL, Wang ZQ, Song D, Fang MY. Anti-cancer effects of Polyphyllin I: an update in 5 years. Chem Biol Interact. 2020;316:108936.
40. Ni B, Wang W, Liu M, Xu Y, Zhao J. Paris saponin I induce toxicity in zebrafish by up-regulation of p53 pathway and down-regulation of wnt pathway. Toxicon. 2023;228:107094.
41. Sun AM, Wang YX, Hu GX, Li L, Wang RR. Polyphyllin I effects candida albicans via inhibition of virulence factors. Evid Based Complement Alternat Med. 2023;2023:5645500.
42. Wang W, Liu Y, Sun M, Sai N, You L, Dong X, et al. Hepatocellular toxicity of paris saponins I, II, VI and VII on two kinds of hepatocytes-HL-7702 and HepaRG cells, and the underlying mechanisms. Cells. 2019. https://doi.org/10.3390/cells8070690.
43. Li Z, Fan Q, Chen M, Dong Y, Li F, Wang M, et al. The interaction between polyphyllin I and SQLE protein induces hepatotoxicity through SREBP-2/HMGCR/SQLE/LSS pathway. J Pharm Anal. 2023;13(1):39–54.
44. Wang JB, Jin Y, Wu P, Liu Y, Zhao WJ, Chen JF, et al. Tumor suppressor PLZF regulated by lncRNA ANRIL suppresses proliferation and epithelial mesenchymal transformation of gastric cancer cells. Oncol Rep. 2019;41(2):1007–18.
45. Han H, Wang S, Meng J, Lyu G, Ding G, Hu Y, et al. Long noncoding RNA PART1 restrains aggressive gastric cancer through the epigenetic silencing of PDGFB via the PLZF-mediated recruitment of EZH2. Oncogene. 2020;39(42):6513–28.
46. Hsieh CL, Botta G, Gao S, Li T, Van Allen EM, Treacy DJ, et al. PLZF, a tumor suppressor genetically lost in metastatic castration-resistant prostate cancer, is a mediator of resistance to androgen deprivation therapy. Cancer Res. 2015;75(10):1944–8.
47. Shen H, Zhan M, Zhang Y, Huang S, Xu S, Huang X, et al. PLZF inhibits proliferation and metastasis of gallbladder cancer by regulating IFIT2. Cell Death Dis. 2018;9(2):71.
48. Feng J, Dai W, Mao Y, Wu L, Li J, Chen K, et al. Simvastatin re-sensitizes hepatocellular carcinoma cells to sorafenib by inhibiting HIF-1α/PPAR-γ/PKM2-mediated glycolysis. J Exp Clin Cancer Res. 2020;39(1):24.
49. Ishtiaq SM, Arshad MI, Khan JA. PPARγ signaling in hepatocarcinogenesis: mechanistic insights for cellular reprogramming and therapeutic implications. Pharmacol Ther. 2022;240:108298.
50. Ning Z, Guo X, Liu X, Lu C, Wang A, Wang X, et al. USP22 regulates lipidome accumulation by stabilizing PPARγ in hepatocellular carcinoma. Nat Commun. 2022;13(1):2187.
51. Wang S, Zhou Y, Yu R, Ling J, Li B, Yang C, et al. Loss of hepatic FTCD promotes lipid accumulation and hepatocarcinogenesis by upregulating PPARγ and SREBP2. JHEP Rep. 2023;5(10):100843.
52. Zhang Q, Xiong L, Wei T, Liu Q, Yan L, Chen J, et al. Hypoxia-responsive PPARGC1A/BAMBI/ACSL5 axis promotes progression and resistance to lenvatinib in hepatocellular carcinoma. Oncogene. 2023;42(19):1509–23.
53. Zuo Q, He J, Zhang S, Wang H, Jin G, Jin H, et al. PPARγ coactivator-1α suppresses metastasis of hepatocellular carcinoma by inhibiting warburg effect by PPARγ-dependent WNT/β-catenin/pyruvate dehydrogenase kinase isozyme 1 axis. Hepatology. 2021;73(2):644–60.
54. Katoch S, Sharma V, Patial V. Peroxisome proliferator-activated receptor gamma as a therapeutic target for hepatocellular carcinoma: experimental and clinical scenarios. World J Gastroenterol. 2022;28(28):3535–54.
55. Wang J, Chu H, Wang Z, Wang X, Liu X, Song Z, et al. In vivo study revealed pro-tumorigenic effect of CMTM3 in hepatocellular carcinoma involving the regulation of peroxisome proliferator-activated receptor gamma (PPARγ). Cell Oncol. 2023;46(1):49–64.
56. Zhao Y, Tan H, Zhang X, Zhu J. Roles of peroxisome proliferator-activated receptors in hepatocellular carcinoma. J Cell Mol Med. 2023;28(5):e18042.
57. Fu S, He K, Tian C, Sun H, Zhu C, Bai S, et al. Impaired lipid biosynthesis hinders anti-tumor efficacy of intratumoral iNKT cells. Nat Commun. 2020;11(1):438.
58. Ibba ML, Ciccone G, Rotoli D, Coppola G, Fiorelli A, Catuogno S, et al. STAT3 silencing by an aptamer-based strategy hampers the crosstalk between NSCLC cells and cancer-associated fibroblasts. Mol Ther Nucleic Acids. 2023;32:111–26.
59. Luo K, Yang L, Yan C, Zhao Y, Li Q, Liu X, et al. A dual-targeting liposome enhances triple-negative breast cancer chemoimmunotherapy through inducing immunogenic cell death and inhibiting STAT3 activation. Small. 2023. https://doi.org/10.1002/smll.202302834.
60. Datta J, Dai X, Bianchi A, De Castro SI, Mehra S, Garrido VT, et al. Combined MEK and STAT3 inhibition uncovers stromal plasticity by enriching for cancer-associated fibroblasts with mesenchymal stem cell-like features to overcome immunotherapy resistance in pancreatic cancer. Gastroenterology. 2022;163(6):1593–612.
61. Stalnecker CA, Coleman MF, Bryant KL. Susceptibility to autophagy inhibition is enhanced by dual IGF1R and MAPK/ERK inhibition in pancreatic cancer. Autophagy. 2022;18(7):1737–9.
62. Kam AE, Masood A, Shroff RT. Current and emerging therapies for advanced biliary tract cancers. Lancet Gastroenterol Hepatol. 2021;6(11):956–69.
63. Deng R, Zhang HL, Huang JH, Cai RZ, Wang Y, Chen YH, et al. MAPK1/3 kinase-dependent ULK1 degradation attenuates mitophagy and promotes breast cancer bone metastasis. Autophagy. 2021;17(10):3011–29.
64. Zhang L, Anglesio MS, O'Sullivan M, Zhang F, Yang G, Sarao R, et al. The E3 ligase HACE1 is a critical chromosome 6q21 tumor suppressor involved in multiple cancers. Nat Med. 2007;13(9):1060–9.
65. Liu Z, Chen P, Gao H, Gu Y, Yang J, Peng H, et al. Ubiquitylation of autophagy receptor optineurin by HACE1 activates selective autophagy for tumor suppression. Cancer Cell. 2014;26(1):106–20.

Publisher's Note